(Received 12 April 2025, Accepted 9 June 2025, Scheduled 21 June 2025)

Design and Analysis of a Half-Mode SSPP Transmission Line for Size Miniaturization

Wang Xu and Lin Li*

The Key Laboratory of Intelligent Textile and Flexible Interconnection of Zhejiang Province
School of Information Science and Engineering, Zhejiang Sci-Tech University, Hangzhou 310018, China

ABSTRACT: By utilizing the symmetry of the field distribution of a coplanar waveguide (CPW) SSPP transmission line (TL), a half-mode SSPP (HMSSPP) transmission line (TL) is presented. Through electromagnetic simulations, it is demonstrated that the proposed HMSSPP TL has a lower asymptotic frequency than the CPW SSPP TL, while occupying only half of the size. Through equivalent circuit analysis, the miniaturization mechanism of the half-mode structure is revealed, and the method to further reduce the asymptotic frequency has been developed. The fabricated and measured HMSSPP TLs confirm the effectiveness and benefits of the half-mode transmission line, achieving significant size reduction and maintaining low insertion loss. Such compact transmission lines are particularly advantageous in space-constrained applications such as portable communication devices, radar systems, and compact RF modules for wireless sensing.

1. INTRODUCTION

Spoof Surface Plasmon Polaritons (SSPPs) are a special type of surface electromagnetic wave that propagates along a dielectric-metal interface and exhibits exponential decay [1]. Characterized by their high field restraint ability, low transmission loss, and flexible dispersion feature, SSPPs are highly favored by researchers. They have found extensive applications in various devices, such as antennas [2, 3], filters [4, 5], transmission lines [6], and sensors [7–11]. However, most of these SSPP devices usually require larger sizes, which limits the practical application of SSPPs to some extent.

A new CPW SSPP with a simple and efficient mode conversion structure is proposed in [12], which effectively reduces transversal width. However, a larger groove depth is still required to confine the field. Many CPW SSPPs with variously shaped top grooves [13–15] and bottom structures [12, 16] have been proposed to further reduce the size. In comparison with other methods for size miniaturization, half-mode components are desirable because they exhibit similar properties to their full-mode counterparts while occupying only half of the size. Consequently, half-mode components are utilized to substitute their full-mode counterparts in many symmetrical configurations [17–19]. However, to the best of our knowledge, half-mode concept has not been applied in the miniaturization of CPW SSPPs.

In this paper, half-mode concept has been applied in conventional CPW SSPP TL featuring folded L-shaped grooves and an interdigital configuration. Equivalent circuits are developed to analyze the dispersion properties of the half-mode SSPP. The performance of the optimized half-mode SSPP TL is verified experimentally. The results show that the designed SSPP TL exhibits compact size, which is beneficial to the miniaturization of the SSPP devices.

2. THEORY AND DESIGN PRINCIPLE

2.1. Half-Mode SSPP Unit Cell

Figures 1(a) and 1(b) respectively display the conventional SSPP unit cell in [11] and its electric field distribution at 2 GHz. It can be observed that its electric field distribution is symmetrical due to the symmetry of the SSPP unit cell. By placing the magnetic wall at the vertical symmetry plane, the half-mode SSPP (HMSSPP) unit cell can be obtained.

Figure 2(a) depicts the layout of the HMSSPP unit cell proposed in this research. Compared to SSPP unit cell, HMSSPP unit cell's central strip comprises an asymmetrical coplanar stripline with the width set to $w_{Hm} = \frac{1}{2}w_{Fm}$. Figure 2(b) displays the electric field distribution of the HMSSPP unit cell at 2 GHz. This distribution pattern suggests that the magnetic wall is maintained on the open side of the HMSSPP unit cell.

To illustrate the role of the bottom interdigital structure, Figure 3 shows the electric field distributions at the bottom of two types of SSPP unit cells. A comparison reveals that the presence of this structure enhances the electric field, which can be represented as a capacitance in the equivalent circuit.

Figure 4 compares the dispersion feature of the HMSSPP and its corresponding full-mode SSPP. As expected, the two dispersion curves agree well, which confirms the effectiveness of the half-mode concept.

2.2. Theoretical Analysis

To further investigate the effects of the HMSSPP, Figure 5 develops the equivalent circuits for both the full- and half-mode

* Corresponding author: Lin Li (lilin_door@hotmail.com).

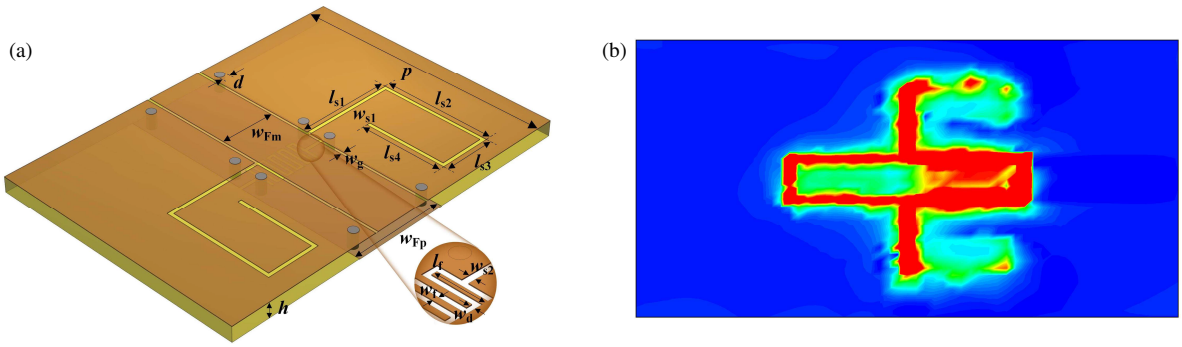

FIGURE 1. (a) Schematic of conventional SSPP unit cell and (b) its E-field distribution.

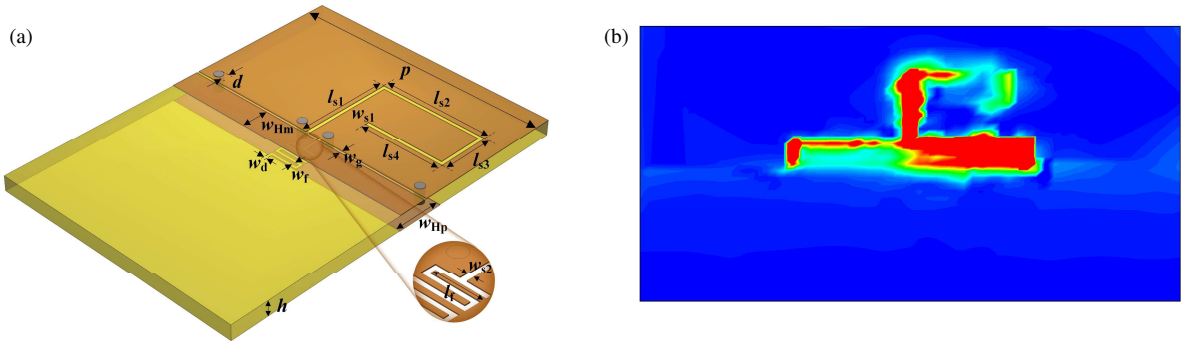

FIGURE 2. (a) Schematic of HMSSPP unit cell and (b) its E-field distribution.

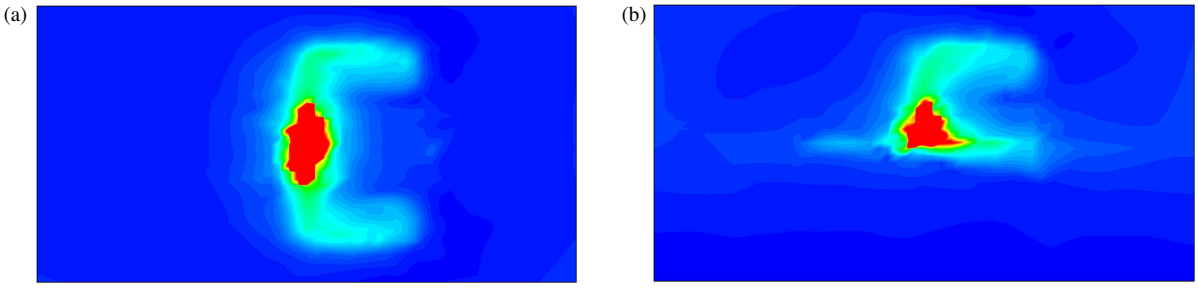

FIGURE 3. E field distributions at the bottom of two types of SSPP unit cells, (a) conventional SSPP, (b) HMSSPP.

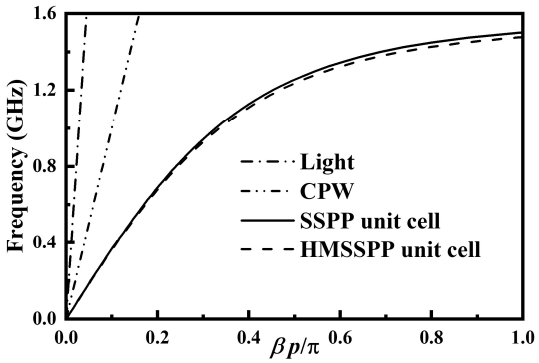

FIGURE 4. Comparison of dispersion curves of different structures. ($w_{Fm} = 3.1$, $w_{Hm} = 1.55$, $w_g = 0.15$, $w_{s1} = 0.2$, $w_{Fp} = 5.2$, $w_{Hp} = 2.6$, $w_{s2} = 0.2$, $w_f = 0.2$, $w_d = 0.2$, $l_{s1} = 5.2$, $l_{s2} = 6$, $l_{s3} = 2.9$, $l_{s4} = 4.5$, $l_f = 1.5$, $p = 13$, $d = 0.5$, $h = 0.8$, unit: mm).

SSPP unit cells. In each unit cell, the ground CPW (GCPW), slot line, and interdigital structure are respectively modeled by the transmission lines, transmission lines, and capacitors. The electromagnetic coupling between the GCPW and slot line is modeled by transformers, with n indicating the coupling coefficient.

For periodic structures, their propagation constant β and dispersion feature are related to the $ABCD$ matrix of the unit cell as follows:

$$\cos \beta p = A \tag{1}$$

Considering the equivalent circuit depicted in Figure 5(a) as a cascade of three simple circuits, its $ABCD$ matrix can be derived by multiplying the $ABCD$ matrices of the individual simple circuits, and then combining (1) to arrive at the following equation:

$$\beta_F p = \cos^{-1}\left(\cos 2\theta_F - \frac{n_F^2 \sin 2\theta_F \cdot Z_S \tan\theta_S}{2Z_F\left(2 - \omega C_F \cdot Z_S \tan\theta_S\right)}\right) \tag{2}$$

Similarly, for Figure 5(b):

$$\beta_H p = \cos^{-1}\left(\cos 2\theta_H - \frac{n_H^2 \sin 2\theta_H \cdot Z_S \tan\theta_S}{2Z_H\left(1 - \omega C_H \cdot Z_S \tan\theta_S\right)}\right) \tag{3}$$

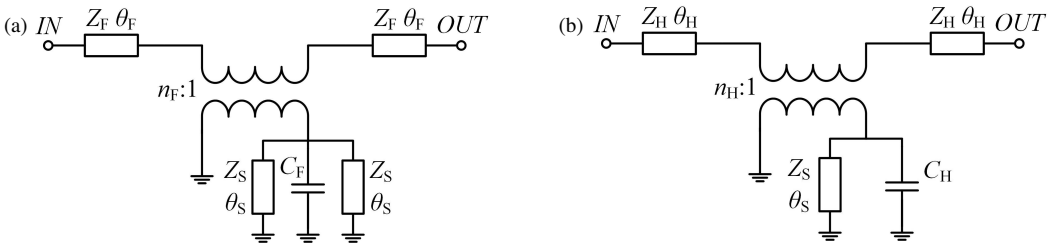

FIGURE 5. The equivalent circuit of each unit cell. (a) SSPP, (b) HMSSPP.

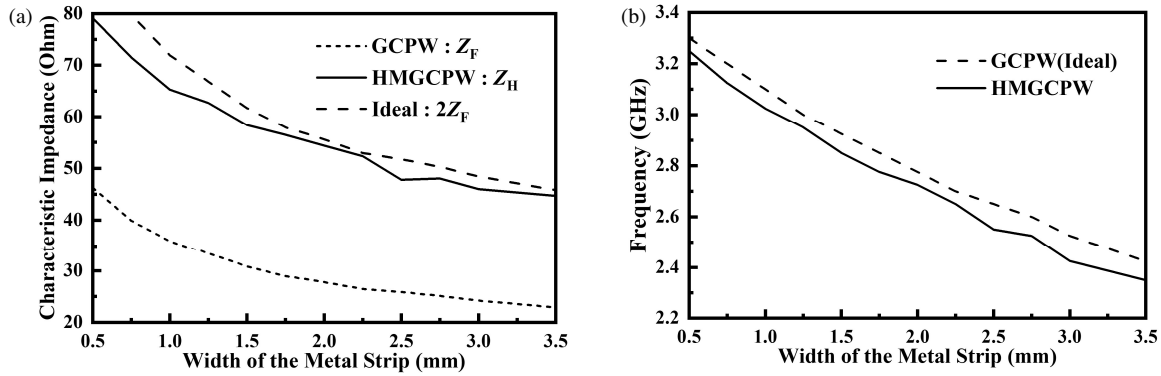

FIGURE 6. (a) Schematic of HMSSPP unit cell and (b) its E-field distribution.

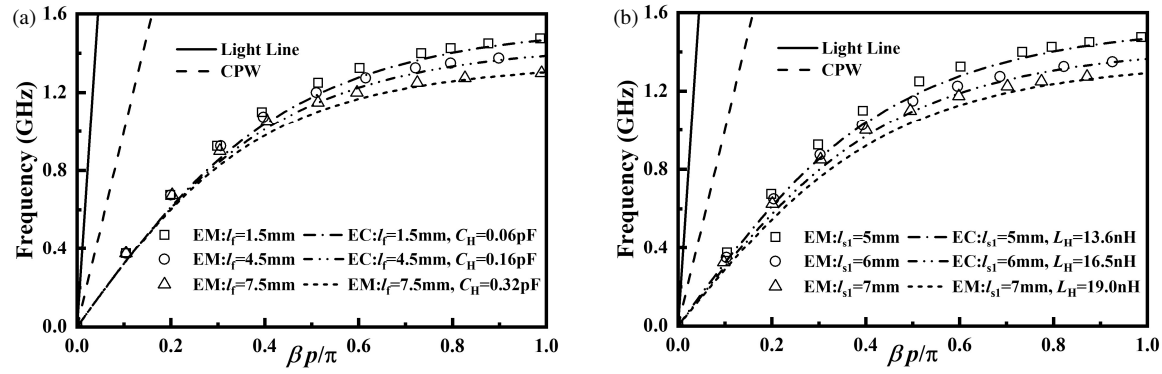

FIGURE 7. Effect of dimensional variations on the asymptotic frequency of the HMSSPP unit cell, (a) slot-line length, (b) interdigital structure length EM: electromagnetic simulation; EC: equivalent circuit.

Obviously, it can be derived from (2) and (3) that half-mode and full-mode SSPPs exhibit the same dispersion feature if: $n_H = n_F$, $C_H = \frac{1}{2}C_F$, $Z_H = 2Z_F$, and $\theta_H = \theta_F$. Considering that the asymptotic frequency of the HMSSPP unit cell is slightly lower than that of the SSPP unit cell in Figure 4, Figure 6(a) displays the relationship between the characteristic impedance of the half-mode GCPW (HMGCPW) and its corresponding GCPW as the metal strip width varies, and Figure 6(b) studies the relationship between their frequency and metal strip width when the electrical length is 90°. In both Figure 6(a) and Figure 6(b), the curves of the HMGCPW are always below the ideal curves; in other words, $Z_H < 2Z_F$ and $\theta_H > \theta_F$. As derived in [11] and (2), both of these factors contribute to a reduction in asymptotic frequency, which provides a reasonable explanation for the lower dispersion asymptotic frequency exhibited by the half-mode SSPP in Figure 4.

To investigate the effect of the dimensional configuration of the HMSSPP unit cell on its performance, Figure 7(a) shows the influence of the slot-line length on the asymptotic frequency. All geometric parameters are kept the same as those in Figure 4, except that l_{s3} increases by the same amount as l_{s1}. Figure 7(b) examines the impact of the interdigital structure length. From the perspective of the equivalent circuit, increasing either of these lengths leads to a larger corresponding inductance or capacitance, resulting in a lower asymptotic frequency, which is consistent with (3).

Additionally, (3) indicates that a decrease in Z_H, an increase in θ_H or C_H results a lower asymptotic frequency, thereby offering a clear direction for optimization. Specifically, this study undertakes the optimization of these parameters by appropriately increasing the width of the HMGCPW and the number of bottom fingers to reduce the asymptotic frequency. This single-

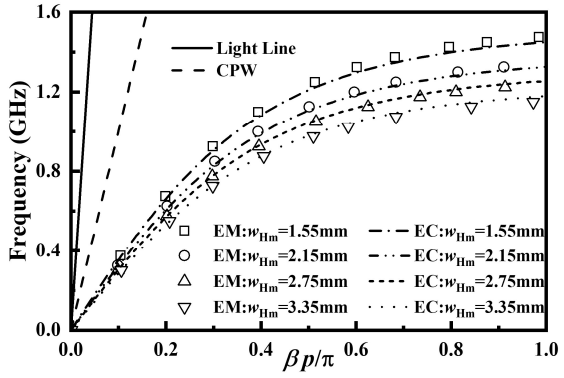

FIGURE 8. Dispersion curves of HMSSPP unit cells with different geometric configurations. EM: electromagnetic simulation; EC: equivalent circuit.

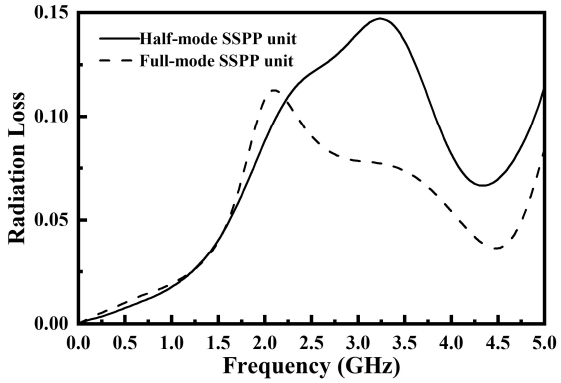

FIGURE 9. Comparison of radiation loss between the HMSSPP unit and the SSPP unit.

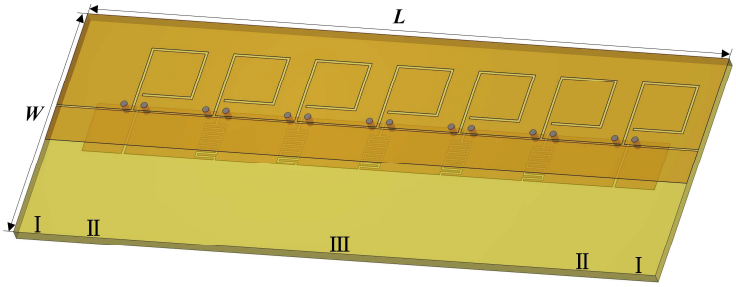

FIGURE 10. Schematic diagram of the HMSSPP TL structure. (Obtained sequentially according to the design steps: $h = 0.8$, $w_{Hm} = 3$, $w_g = 0.15$, $w_{Hp} = 4.3$, $w_{s1} = 0.2$, $p = 13$, $l_{s1} = 5.7$, $l_{s2} = 4.5$, $l_{s3} = 4.4$, $l_{s4} = 4$, $w_{s2} = 0.2$, $w_f = 0.17$, $w_d = 0.15$, $l_f = 1.5$, $d = 0.5$, $L = 51$, $W = 20$, unit: mm.).

dimension increase results in a three-fold optimization, demonstrating remarkable efficiency. Figure 8 presents the simulation outcomes for this procedure, covering four separate metal strip widths: 1.55 mm, 2.15 mm, 2.25 mm, and 3.35 mm. The transmission line electrical parameters corresponding to their equivalent circuits can be inferred from Figure 6. The remaining parameters are as follows: $n_H = 0.85$, $Z_S = 117.4\,\Omega$, $\theta_S = 90°$ at 2.62 GHz with the corresponding C_H values being: 0.06 pF, 0.08 pF, 0.10 pF, and 0.12 pF, respectively.

However, the half-mode structure inevitably introduces additional radiation loss. Figure 9 shows a comparison of the radiation loss between the HMSSPP unit and SSPP unit based on the method in [20]. It can be observed that although the introduction of the half-mode structure increases radiation loss, the difference between the two is minor below the asymptotic frequency of $f_a = 1.5$ GHz.

In summary, the HMSSPP TL retains all the advantages of the SSPP TL, while achieving a lower asymptotic frequency and half of the size, enhancing its potential for microwave system miniaturization.

3. FABRICATION AND MEASUREMENT

The design process for the HMSSPP on a predetermined FR4 substrate, with a loss tangent of 0.02 and a dielectric constant of 4.4, based on (3) and the desired asymptotic frequency, is as follows:

1. Specify the desired asymptotic frequency $f_a = 1.2$ GHz.

2. Set $Z_H = 50\,\Omega$ and determine the width of the HMGCPW, which can be obtained by halving the $Z_F = 25\,\Omega$ GCPW.

3. Select a narrower slotline with $w_{s1} = 0.2$ mm to reduce radiation loss, which corresponds to $Z_S = 117.4\,\Omega$.

4. Determine θ_H and θ_S according to the desired longitudinal length and transversal width of the unit. In this design, $\theta_H = 22.5°$ and $\theta_S = 41.5°$ at f_a.

5. Obtain the transformer's turn ratio $n = 0.85$ using the method given in [21].

6. Calculate $C_H = 0.15$ pF using (3) and obtain the dimensions of the interdigital structure.

7. Optimize the HMSSPP unit dimensions as necessary.

8. Cascade multiple HMSSPP units and design the transition to improve impedance matching if needed.

Figure 10 displays the schematic diagram of the design, which consists of three parts: (I) HMCPW serving as the input/output ports, (II) a transition zone without interdigital structures, and (III) five periodic proposed HMSSPP unit cells. Figure 11 shows the fabricated transmission line.

Figure 12 displays the simulated and measured S-parameter curves, which exhibit good agreement. The differences between the simulated and measured results may be attributed to fabrication tolerances and the measurement environment.

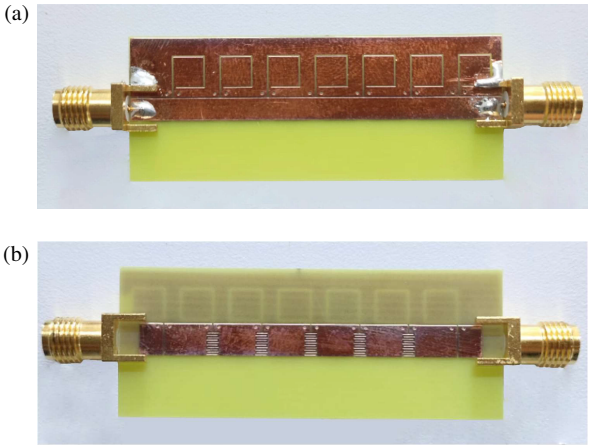

FIGURE 11. The physical photo of the fabricated HMSSPP TL. (a) Top view. (b) Bottom view.

Table 1 compares some reported SSPP TLs with the HMSSPP TL. The proposed HMSSPP TL is more compact in both transversal width w_t and period p.

TABLE 1. Performance of previous works and this work.

Ref.	f_a (GHz)	$w_t(\lambda_a)$	IL (dB)	$p(\lambda_a)$
[2]	12.54	0.177	3	0.084
[5]	5.06	0.192	1.4	0.245
[12]	8.9	0.160	4	0.119
[13]	3.8	0.263	1.1	0.032
[14]	1.78	0.083	3	0.044
[16]	1.81	0.071	2	0.042
[22]	16	> 0.48	2.5	0.053
This work	**1.21**	**0.036**	**1.4**	**0.026**

f_a: the asymptotic frequency, λ_a: the wavelength at f_a, w_t: the transversal width, p: the period.

4. CONCLUSION

In this paper, the HMSSPP TL is proposed, and the equivalent circuit provides a solid theoretical explanation for size reduction mechanism. The experimental results show that the design significantly reduces the size of the prototype SSPP TL. The half-mode concept can be further utilized in other SSPPs to obtain size reduction. Moreover, the measured low insertion loss demonstrates that the proposed miniaturized design does not compromise transmission performance. The proposed HMSSPP TL holds promise for integration into portable microwave devices, real-time sensing modules, and space-constrained wireless systems, contributing to the development of practical, miniaturized radio frequency (RF) and microwave solutions.

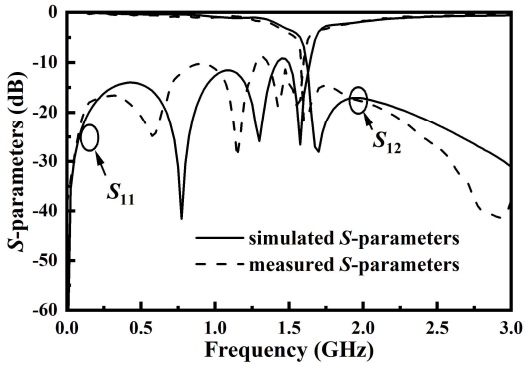

FIGURE 12. Simulation and measurement results of S-parameter of HMSSPP TL.

REFERENCES

[1] Pendry, J. B., L. Martin-Moreno, and F. J. Garcia-Vidal, "Mimicking surface plasmons with structured surfaces," *Science*, Vol. 305, No. 5685, 847–848, 2004.

[2] Ye, L., Z. Wang, J. Zhuo, F. Han, W. Li, and Q. H. Liu, "A backfire to forward wide-angle beam steering leaky-wave antenna based on SSPPs," *IEEE Transactions on Antennas and Propagation*, Vol. 70, No. 5, 3237–3247, 2022.

[3] Wen, L., W. Hu, B. Pang, Q. Luo, and S. Gao, "Spoof surface plasmon polariton-based antenna and array by exciting both even- and odd-mode resonances," *IEEE Transactions on Antennas and Propagation*, Vol. 72, No. 2, 1593–1602, 2024.

[4] Liu, Y., K.-D. Xu, J. Li, Y.-J. Guo, A. Zhang, and Q. Chen, "Millimeter-wave E-plane waveguide bandpass filters based on spoof surface plasmon polaritons," *IEEE Transactions on Microwave Theory and Techniques*, Vol. 70, No. 10, 4399–4409, 2022.

[5] Pan, L., Y. Wu, W. Wang, Y. Wei, and Y. Yang, "A flexible high-selectivity single-layer coplanar waveguide bandpass filter using interdigital spoof surface plasmon polaritons of bow-tie cells," *IEEE Transactions on Plasma Science*, Vol. 48, No. 10, 3582–3588, 2020.

[6] Xu, H., W.-S. Zhao, D.-W. Wang, and J. Liu, "Compact folded SSPP transmission line and its applications in low-pass filters," *IEEE Photonics Technology Letters*, Vol. 34, No. 11, 591–594, 2022.

[7] Kandwal, A., Z. Nie, T. Igbe, J. Li, Y. Liu, L. W. Y. Liu, and Y. Hao, "Surface plasmonic feature microwave sensor with highly confined fields for aqueous-glucose and blood-glucose measurements," *IEEE Transactions on Instrumentation and Measurement*, Vol. 70, 1–9, 2020.

[8] Imamvali, S., S. Rajak, and S. Tupakula, "Plasmonic waveguide with spoof localized plasmon polariton based resonator for biosensing applications," in *2024 International Conference on Microelectronics (ICM)*, 1–6, Doha, Qatar, Dec. 2024.

[9] Imamvali, S., K. Prakash, S. Bansal, S. Tupakula, A. K. Suresh, A. J. A. Al-Gburi, M. R. I. Faruque, and K. S. Al-mugren, "Label-free biosensing of persistent organic pollutants in sewage water using spoof surface plasmon polaritons," *Sensors and Actuators A: Physical*, Vol. 388, 116504, 2025.

[10] Imamvali, S., T. Nagarajan, R. Chaparala, and S. Tupakula, "Spoof surface plasmon polaritons based detection of glucose in blood phantom for medical diagnosis," *IEEE Sensors Journal*, Vol. 24, No. 23, 38 952–38 961, 2024.

[11] Imamvali, S., R. Chaparla, S. Tupakula, and D. Chaturvedi, "Novel SSPP sensor system with octagon-shaped unit cell for liquid analyte dielectric constant detection," in *2023 Photonics & Electromagnetics Research Symposium (PIERS)*, 1467–1473, Prague, Czech Republic, Jul. 2023.

[12] Li, J., J. Shi, K.-D. Xu, Y.-J. Guo, A. Zhang, and Q. Chen, "Spoof surface plasmon polaritons developed from coplanar waveguides in microwave frequencies," *IEEE Photonics Technology Letters*, Vol. 32, No. 22, 1431–1434, 2020.

[13] Cao, Y., Y. Lu, S. Yin, and X. Hu, "A CPW-based novel SSPP reflectionless low-pass notch filter with loaded interdigitated coupling structure," *IEEE Access*, Vol. 12, 117863–117871, 2024.

[14] Wang, C.-M., W. Xu, L. Li, H. Liu, and Y. Kuang, "Capacitor-loaded coplanar waveguide spoof surface plasmon polariton with reduced transversal width," *IEEE Photonics Technology Letters*, Vol. 35, No. 10, 557–560, 2023.

[15] Chaparala, R., S. Imamvali, and S. Tupakula, "Enhancement of spoof surface plasmon polariton waveguide performance through modified groove width," *Optical Engineering*, Vol. 63, No. 5, 055102, 2024.

[16] Cao, R.-F., L. Li, and H.-W. Liu, "Compact CPW spoof surface plasmon polariton transmission line with interdigital structure," *IEEE Photonics Technology Letters*, Vol. 35, No. 24, 1427–1430, 2023.

[17] Hong, W., B. Liu, Y. Wang, Q. Lai, H. Tang, X. X. Yin, Y. D. Dong, Y. Zhang, and K. Wu, "Half mode substrate integrated waveguide: A new guided wave structure for microwave and millimeter wave application," in *2006 Joint 31st International Conference on Infrared Millimeter Waves and 14th International Conference on Teraherz Electronics*, 219–219, Shanghai, China, Sep. 2006.

[18] Liu, F.-X., Z. Xu, D. C. Ranasinghe, and C. Fumeaux, "Textile folded half-mode substrate-integrated cavity antenna," *IEEE Antennas and Wireless Propagation Letters*, Vol. 15, 1693–1697, 2016.

[19] Lu, J., J. Wang, and H. Gu, "Design of compact balanced ultra-wideband bandpass filter with half mode dumbbell DGS," *Electronics Letters*, Vol. 52, No. 9, 731–732, 2016.

[20] Han, C., D. Tang, Z. Deng, H. J. Qian, and X. Luo, "Filtering power divider with ultrawide stopband and wideband low radiation loss using substrate integrated defected ground structure," *IEEE Microwave and Wireless Components Letters*, Vol. 31, No. 2, 113–116, 2021.

[21] Caloz, C., H. Okabe, T. Iwai, and T. Itoh, "A simple and accurate model for microstrip structures with slotted ground plane," *IEEE Microwave and Wireless Components Letters*, Vol. 14, No. 3, 127–129, 2004.

[22] Guan, D.-F., P. You, Q. Zhang, Z.-B. Yang, H. Liu, and S.-W. Yong, "Slow-wave half-mode substrate integrated waveguide using spoof surface plasmon polariton structure," *IEEE Transactions on Microwave Theory and Techniques*, Vol. 66, No. 6, 2946–2952, 2018.